Dynamic simulation of particle self-assembly applied to microarray technology

Vito Di Virgilio, Arnau Coll, Sandra Bermejo and Luis Castañer
MNT - Micro and Nano Technology Group
ETSEIB Universitat Politècnica de Catalunya, Barcelona (Spain)
*Corresponding author: vito@eel.upc.edu

Abstract:
In this work we want to explore some techniques, microfluidic and electrospray-ionization based, suitable for dynamic microarrays' fabrication.

The fabrication techniques are based on manipulation and self-assembly of selective coated micro and nanobeads. The simulation will include electro-osmotic flow, species transport, and electrostatics.

Keywords: self-assembly, micro/nano-particles, micro/nano-beads electrospray, ESI, microfluidics, dielectrophoresys, dynamic microarrays.

1. Introduction

Microarray is a multiplex technology widely used in medicine and biology for fast detection of drugs, DNA sequencing, protein detection etc. It is composed by a 2D matrix of thousand of spots, picoliter sized, of different reagents [1].

The spots are equally spaced, a hundred of microns gap, and generally are obtained by dip-pen. The detection can be done once and it is based on photoluminescence, therefore it suffers photobleaching and quenching problems. Recent developments of microarray technology go towards reusable devices [2]. This technology is based on biomaterial-coated micro and nano beads.

A bottom-up approach is suitable for placing coated beads [6] in the desired sites and self-assembly seems to be a good candidate [3,4,5].

Microarray can be classified in two main categories: static and dynamic. Static microarrays are based on immobilizing biomolecules and chemicals directly on the solid surface of the support, in microspots.

The fabrication is relatively easy and it can be done by high speed arrayer printing on glass slides [7], photolithography, using micromirrors [8] or masks [9].

Dynamic microarrays are based on immobilizing biomolecules and chemicals on mobile substrates, usually micro/nano beads [10].

Besides the bead-based ones, dynamic microarrays also include the cell-based ones [11].

In comparison with the static microarrays, dynamic microarrays show a number of advantages: 1. the possibility to mix-and-match beads, in order to select the type of screening to be performed, and introduce them on demand in the circuit; 2. beads can be washed out and replaced, allowing the device to be reused a certain number of times resulting in cost-effectiveness; 3. beads allow much faster reactions (due to the larger surface shown respect to the planar substrate one).

The potential of dynamic microarrays can be fully exploited using a platform for transporting, immobilizing the beads and furthermore detect and observe the optical response.

Here we show simulation studies of two different fabrication techniques for dynamic microarray fabrication.

Both techniques are bead-based and the microarray spots are obtained by beads' self-assembly.

The first technique considered is purely microfluidic and is based on electrostatic trapping and release of the beads. The beads assemble together driven by the electrostatic fields (directed self-assembly). The second fabrication strategy is based on electrospray ionization (ESI) deposition technology.

The particles are deposited using an electrostatic mask to template the posts. The devices fabricated with this technique are cost effective, as the reactive sites can be washed out after use. In addition, ESI technique allows to finely control the deposition of the reagent.

The other important feature is that the devices fabricated by ESI can be post-processed with standard scanners.

2. Theoretical background: modeling of particles' motion

In this section will be discussed the theoretical background of the two fabrication techniques taken into account: microfluidic and ESI.

2.1 Microfluidic: modeling of particles' motion

The microfluidic approach for microarray fabrication is based on a simple Y-shaped microfluidic channel with 2 (or more) inlets and one outlet (made in polydimethylsiloxane - PDMS) patch clamped on the substrate on which the reactive spots have to be deposited. A sketch of the setup is shown in figure 1. The height of the channel is 50 microns, 300microns wide, some centimeters in length.

The substrate to be deposited can be a simple glass slide but it is envisaged the use of flexible polymer sheets in order to get cost effective, biocompatible and flexible device. On this substrate, the only operation to be made is the metallization of the electrodes to be polarized and trap the beads. The PDMS channel has embedded electrodes at the inlet and at the outlet for electrophoresys. The metal to be deposited is ITO (Indium Tin Oxide) in order to preserve the transparency of the device. The functionalized nanobeads will be introduced from one of the inlets and, driven by electrostatic forces, trapped on the ITO electrodes self-assembling in mono and multi layers.

Once the reactive sites are ready(the beads trapped), the main channel is flushed with a buffer solution flow and then filled up with the solution to be analyzed, which starts the reaction with the trapped beads. The collection of the light signal is done by microscopy from the upper or lower side of the microfluidic chip.

The model of the microchannel is approximated to a 2D structure. The nanobeads used in the experiment are made in polystyrene and will measure 100nm in diameter (provided by nanospheres-microspheres.com).

We assume that the sedimentation of the particles due to the gravity is negligeable because the density of the particles ($1.05 g/m^3$) is close to that of the solution.

The solution containing the beads is provided from one of the two (or more) inlets. The beads move by electroosmosys, applying a 5 volts potential across the microchannel.

Assuming the formation of a thin electric double layer (EDL), and no retardation effect, the electrophoretic force acting on a single bead is:

$$\vec{F}_{EP} = 6\pi\varepsilon_B r^3 \xi_P \vec{E} \qquad (1)$$

where ε_B is the permittivity of the liquid buffer, ζ_P the zeta potential of the particle and $\vec{E}$ the induced electric field.

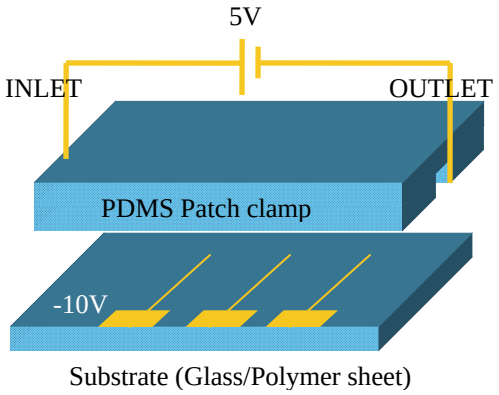

Figure 1. Section of the patch clamping setup: a voltage supply of 5 volts is connected to the inlet and outlet of the PDMS microfluidic chip. The bottom substrate has straight electrodes to act as particle trapping when 10V are applied.

Assuming the velocity of each particle as $\frac{d\vec{r}_P}{dt}$ so according to the Stoke's law a drag force can be written as:

$$\vec{F}_{Drag} = -6\pi\eta a\left(\frac{d\vec{r}_P}{dt} - U_{EOF}\right) \qquad (2)$$

Where η is the dynamic viscosity of the buffer and $U_{EOF} = -\frac{\varepsilon_p \xi_{pdms}}{\eta}\vec{E}$ is fluid velocity due to the electroosmotic flow, which can be estimated from Smoluchowski's equation, being ζ_{pdms} the zeta potential at the walls. For PDMS we assume the zeta potential to be -23.5mV [12].

When the potential is applied to each single bottom electrode, the particles feel a stronger electrophoretic trapping force towards the electrode itself, figure 2. This force traps the beads onto the electrode as shown in figure 3. The beads tend to self assemble in multilayers on the top of the electrodes. The signal collection is currently ensured due to the transparency of the ITO electrode.

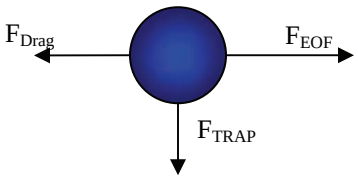

Figure 2. Forces acting on the single polystyrene bead.

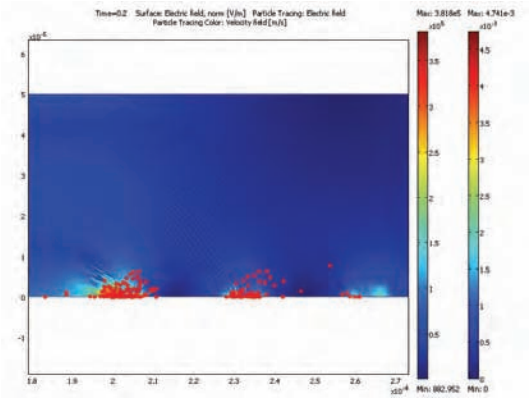

Figure 3. Polystyrene beads trapped by three electrodes, 50 microns wide and separated each other 30 microns.

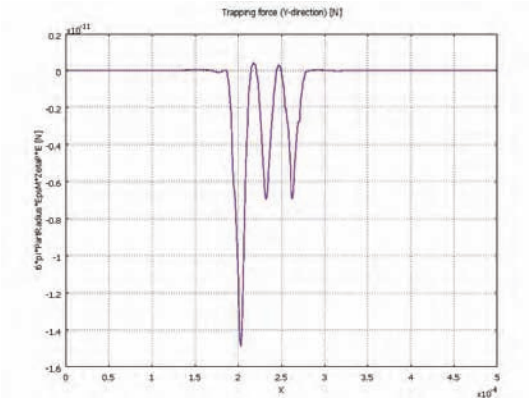

Figure 4. Trapping force (F_{EP} in y-direction) calculated across the bottom surface of the microfluidic chip. The maximum trapping force is 14.8 pN at the first electrode. The following electrodes show 6.88 pN. The first electrode is probably a singularity point and the attractive force results to be higher. Simulations run with more than three electrodes show the same scenario: the closer electrode shows a F_{EP} around 15 pN, the others show a lower attractive force.

Figure 4 shows the trapping electrophoretic force across the bottom surface of the channel. The three negative peaks represents the electrodes, which actually are the trapping sites.

The resulting trapping force is in the range of pico Newtons, 14.8pN for the first electrode and 6.8pN for the second and third. It is interesting to verify that the first electrode generates a stronger electric field than the following electrodes which generates slightly the same trapping force.

Once the beads are trapped onto the electrodes' surface, the flushing operation becomes critical as the hydrodynamic drag force acting on the particles could detach and drag away in the flow the reactive components of the chip.

It is then very important to take in account the maximum flow rate to apply during the flushing and reaction operation.

As the flow is provided by a pump, the hydrodynamic drag force generated will not be as important as the velocity at the edge of the channel should be near to zero (because of the parabolic shape of the velocity field).

Anyway, the force in *x* direction exerted by the electrostatic field on the particle is $8.6e\text{-}12<F_{eofX}<1.65e\text{-}11$, therefore the maximum fluid velocity before the particles' lift off is 4.6 μm/s at the bottom of the channel. At the level of 100nm the parabolic flow exhibits a very low velocity. Nevertheless the flow will be adjusted to 0.001ml/h which produces a maximum velocity at the center of the channel of about 1cm/s. In order to detach the beads it will be necessary to apply a counter voltage to induce the levitation and drag with the flushing flow.

2.2 Electrospray ionization: experimental setup and charged particles' motion

The experimental setup is shown in figure 5. It consists basically in a metal needle (Hamilton Co. 470 μm O.D. and 130 microns I.D., gauge 26s) connected to a high voltage source. A liquid

flow is provided by a medical pump (Infusomat Pump, Braun A.G.).

The substrate to be coated is a simple glass slide for microscope. Between the needle and the glass slide it is placed a nickel mask, figure 6, connected to the high voltage source at a lower voltage in order to provide three effects: 1. it acts as extractor of the fluid out of the needle, creating the so-called Taylor cone; 2. it acts as a particle focus as the particles are forced to reach the lowest potential; 3. the nickel mask acts as a shadow mask in order to tailor the reaction sites one wants to deposit.

The microscope slide is placed on a metal plate connected to the ground. In the simulation we expect to find well defined particles' paths, so the simulations will help us to tune the particles deposition process.

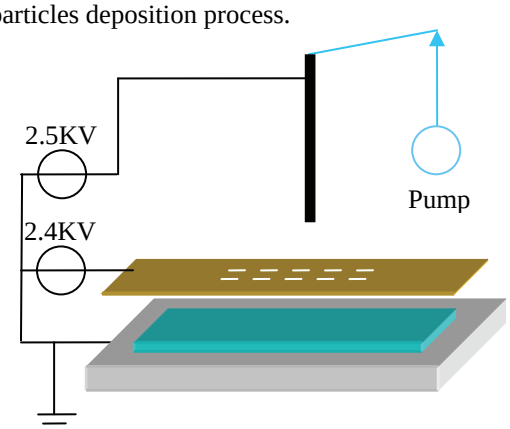

Figure 5. Electrospray setup: the needle is placed close by the mask, which is biased with a lower voltage as an electronic lens. The substrate to be deposited is placed underneath the mask, upon a grounded metal plate. The mask also works as an extractor for the formation of the Taylor cone.

The setup is mounted vertically. To prevent sample contamination in the startup of the deposition process, we placed a shutter connected to ground, in order to collect all the drops of liquid that could spill on the sample. Generally, to prevent this kind of problem, the needle tip is placed 60 degrees tilted respect to the sample. We decided for the most expensive and more reliable solution of the shutter to be sure any drop reaches the sample. The atmosphere is kept dry by providing nitrogen and so helping the liquid to evaporate during the flight time.

The motion of the charged particles is described by the equation:

$$m\frac{d^2\vec{r}(t)}{dt^2} = q\vec{E} - \vec{F}_{drag} \qquad (3)$$

where m is the mass of the droplet and q its charge; F_{drag} is the drag force exerted by the ambient atmosphere on the particle [13]. It is defined as:

$$\vec{F}_{drag} = \frac{1}{2}C_d \rho A \vec{v} \qquad (4)$$

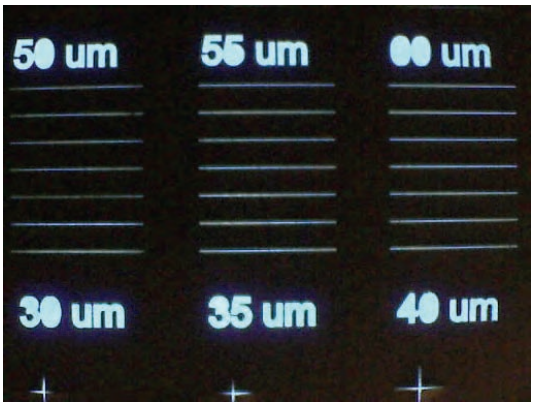

Figure 6. Nickel mask for focusing, driving and centering the particles during deposition.

where ρ is the density of the density of the air, A the cross-section of the droplet and v its velocity. C_D is the so-called drag coefficient, defined as:

$$C_d = \frac{24}{\mathrm{Re}} + \frac{6}{1+\sqrt{\mathrm{Re}}} + 0.4 \qquad (5)$$

and it depends on the Reynold's number $Re=\rho lv/\eta$ where l is the diameter of the droplet and η is the viscosity of air.

The resulting simulation is shown in figure 7. As we can see, the particles are mainly focused to get through the driving holes of the mask.
The resulting deposition is the shadow image of the mask. The key-role of the mask takes place when the difference in potential between the emitting tip and the mask is very small.

This fabrication method results to be cost effective and very rapid. Nevertheless it is necessary to design and fabricate shadow masks.
The accuracy of the deposit depends on the close the mask can get to the deposition surface, the accuracy in fabrication of the mask and

obviously, the quality of the functionalized beads colloid.

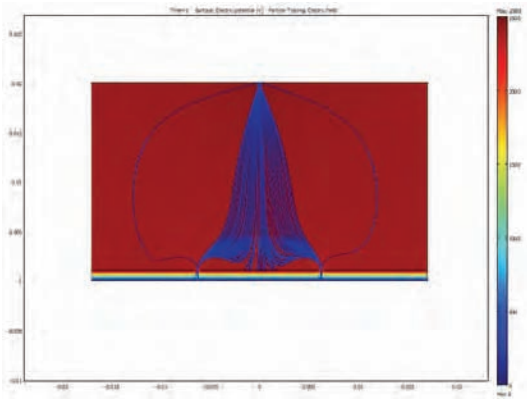

Figure 7 Electrospray particle tracking: the particles are mainly focused in the holes towards the ground beneath the nickel mask polarized with 2.4 KV.

7. Conclusions

The main motivation of this work is to test the feasibility of new microarray fabrication technologies, cost effective and rapid prototyping. The technology based on microfluidic has to be carefully tested in order to tune finely the hydrodynamic flow at the moment of supplying the fluid under test and in the flushing mode, to avoid the lift off of the particles.

This problem is easily solved increasing the voltage applied, nevertheless, bubbles and electrolysis could happen. Low voltage applied also means possibility to make the device portable. In this case the pumping system should be chosen as a micropump (electroosmotic for example). This solution also avoids the lift off due to hydrodynamic drag force. Microfluidics also make possible to dynamically set up microarrays, while the electrospray fabrication based technology only allows to mass produce microarrays very cost effective, and very rapidly, keeping the compatibility with the already existing test and signal collection technology.

8. References

1. Avseenko N.V. et al., Immobilization of proteins in immunochemical microarrays fabricated by electrospray deposition. *Anal Chem.* **73(24)**, 6047-52. (2001);

2. Scott Eastman P. et al., Qdot Nanobarcodes for Multiplexed Gene Expression Analysis, *Nano Lett.*, **6 (5)**, 1059-1064, (2006).

3. Whitesides G.M. et al., Molecular Self-Assembly and Nanochemistry: A Chemical Strategy for the Synthesis of Nanostructures", *Science*, **254,** 1312-1319(1991).

4. Tien J. et al., Microfabrication through Electrostatic Self-Assembly, *Langmuir*, **13**, 5349(1997).

5. Jonaset U. et al., Colloidal assemblies on patterned silane layers, *PNAS*, **99,** 5034, (2002).

6. Filipponi L. et al.. Microbeads on microposts: An inverted architecture for bead microarrays *Biosensors and Bioelectronics***, 24 (7),** 1850-1857(2009).

7. Robinson WH, DiGennaro C et al., Antigen microarrays for multiplex characterization of antibody response, *Nature Medicine,* **8**,295–301 (2002)

8. Singh-Gasson S., Green R.D. et al., Maskless fabrication of light-directed oligonucleotide microarrays using a digital micromirror array, *Nature Biotechnology* **17**, 974–978 (1999).

9. Fodor S.P., Read J.L., Pirrung M.C., Stryer L., Lu A.T., Solas D., Light-directed, spatially addressable parallel chemical synthesis, *Science*, **251**,767–773(1991).

10. Iwai K., Wei-Heong T., Takeuchi S., A resettable dynamic microfluidic device, *Micro Electro Mechanical Systems, 2008. MEMS 2008.*

11. Palmer, E. & Freeman, T. Cell-based microarrays: current progress, future prospects, *Pharmacogenomics*, **6(5),** 527-534 (2005).

12. Ren X., Bachman M. et al., Electroosmotic properties of microfluidic channels composed ofpoly(dimethylsiloxane), *Journal of Chromatography B: Biomedical Sciences and Applications*, **A 762**, 117 (2001).

13. Timmermann P., van der Weele J.P., On the rise and fall of a ball with linear or quadratic, *American Journal of Physics*, **67 (6)**, 538-546(1999).

9. Acknowledgements

This work has been founded by the Spanish Ministry of Science and Innovation with the grant BES-2008-007481 associated to the project TEC2007-67081.